Experimental study of the evanescent-wave photonic sensors response in presence of molecular beacon conformational changes

Ángela Ruiz-Tórtola [1], Francisco Prats-Quílez[1], Daniel Gónzalez-Lucas[2], María-José Bañuls[2], Ángel Maquieira[2], Guy Wheeler[3], Tamas Dalmay[3], Amadeu Griol[1], Juan Hurtado[1], Helge Bohlmann[4], Reiner Götzen[4], Jaime García-Rupérez[1,*]

[1] Nanophotonics Technology Center, Universitat Politècnica de València, Camino de Vera s/n, 46022 Valencia, Spain.
[2] IDM, Instituto Interuniversitario de Investigación de Reconocimiento Molecular y Desarrollo Tecnológico, Departamento de Química, Universitat Politècnica de València, 46022 Valencia, Spain.
[3] School of biological Sciences, University of East Anglia, Norwich Research Park, Norwich, NR4 7TJ, UK
[4] microTEC Gesellschaft für Mikrotechnologie mbH, Duisburg, Germany

An experimental study of the influence of the conformational change suffered by molecular beacon (MB) probes -upon the biorecognition of nucleic acid target oligonucleotides over evanescent wave photonic sensors- is reported. To this end, high sensitivity photonic sensors based on silicon photonic bandgap (PBG) structures were used, where the MB probes were immobilized via their 5' termination. Those MBs incorporate a biotin moiety close to their 3' termination in order to selectively bind a streptavidin molecule to them. The different photonic sensing responses obtained towards the target oligonucleotide detection, when the streptavidin molecule was bound to the MB probes or not, demonstrate the conformational change suffered by the MB upon hybridization, which promotes the displacement of the streptavidin molecule away from the surface of the photonic sensing structure.
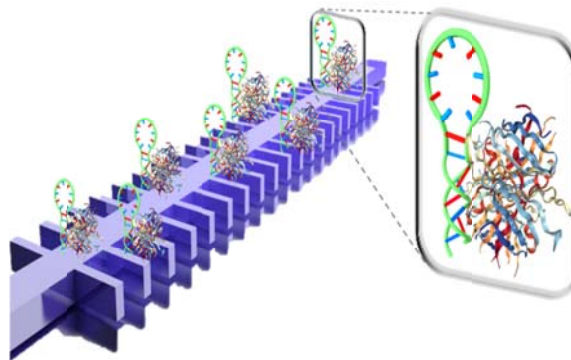
Schematic diagram of the PBG sensing structure on which the streptavidin-labeled MB probes were immobilized.

1. Introduction

The development of new strategies for detecting DNA and RNA strands has become highly interesting for several application fields such as food quality control [1, 2], pathogen detection [3, 4] or biological safety [5]. The detection of DNA/RNA strands is also key in the biomedical field, due to the close link of these molecules to personalized medicine, early disease detection, forensic investigation or assessment of medical treatments, among others [6-13]. Numerous detection systems based on the hybridization between a DNA/RNA target and its complementary strand have been reported up to date, in which typically linear single-stranded DNA probes are used in microarray formats [14, 15].

Given the relevance of the detection of these DNA/RNA targets for bioanalysis and biomedical research, alternative approaches for their recognition have been investigated. Among them, we can highlight the use of MB probes: a special type of nucleic acid with a stem-loop structure where the recognition of the target strand produces a conformational change of the probe itself [16]. The use of fluorophore-labeled MBs in

solution has proven to have high potential for the detection of short sequence nucleic acid strands, also called oligonucleotides [17-19]. Moreover, MBs exhibit an extraordinary stability, a better selectivity and a higher specificity than similar assays performed using linear single-stranded probes [20].

Some examples of heterogeneous assays, where the MBs are immobilized onto a solid substrate, can also be found using a range of optical (e.g. fluorescence [21-24], surface enhanced Raman spectroscopy [25], nanotweezers [26]) and electronic [27] sensing platforms. However, we can find some few works where the conformational change of the MB is used to change its interaction over a transduction element. Typically in those works, a particle/molecule, able to interact with an electrochemical transducer, is attached to the MB probe, so that a variation in the measured electrical signal is produced when that particle/molecule is displaced due to the conformational change of the MB after hybridization [28-31]. Those works demonstrate the high potential of exploiting the hairpin conformational changes of MBs upon hybridization changing the interaction of a given molecule/particle with a transduction element, that can open the door to the development of high performance MB-based biosensing devices.

Within this context, we report an experimental demonstration of the influence of the conformational change of molecule-labeled MB probes over an evanescent wave photonic sensing structure. Despite this mechanism has been demonstrated for electrochemical transduction approaches, as previously indicated, this is to our knowledge the first time that this effect is observed for evanescent wave photonic sensors.

2. Molecular Beacon detection scheme

When a MB hybridizes with its complementary strand, it undergoes a conformational change opening the stem and adopting the typical double helix configuration [32, 33]. The most common exploitation of MB probes consists of a hairpin probe structure with a fluorophore (reporter) and a quencher on each end. Then, the hybridization promotes the separation of the quencher away from the reporter, restoring the fluorescence, as depicted in Figure 1 [16]. Despite the widespread use of the described fluorescence-based MB configuration for oligonucleotide detection in homogenous assays [21-24], its performance is limited by the difficulty of detecting the small fluorescence changes produced by small oligonucleotide concentrations.

In the present work, the MB design is adapted in order to provide a simple and versatile way of anchoring any potential labeled MB to a given photonic sensor. The modified MB design includes a thiol termination on the 5' end, for the immobilization on the photonic sensing structure, and a biotin moiety close to the 3' end,

allowing the incorporation of a streptavidin (St) molecule to the MB [34], as shown in Figure 2. The biorecognition of the target oligonucleotide by the streptavidin-labeled MB probe will induce a change in the response of the photonic sensing structure due to both the hybridization and conformational change of the MB probe, which will displace the streptavidin molecule away from the surface of the photonic sensing structure. That response of the photonic sensor having streptavidin-labeled MB probes will be compared with the case when streptavidin-free MB probes are used in order to determine the influence of the displacement of the molecule on the optical sensing response.
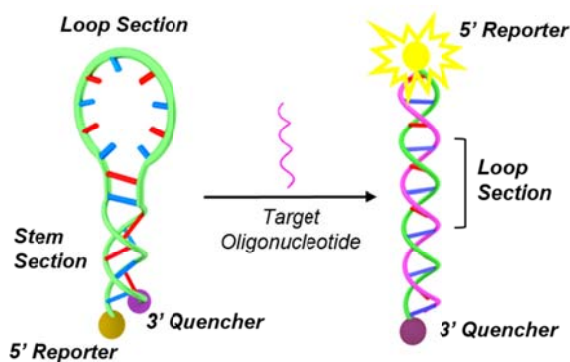

Figure 1 Schematic explanation of the working principle of a fluorescence-based MB probe for oligonucleotide detection.

Figure 2 Scheme of the hybridization events for the streptavidin-free and the streptavidin-labeled MB probes being immobilized on the surface of a photonic structure.

Conformational changes and protein-surface distances of streptavidin-labeled MB upon hybridization were previously reported by our group based on dual polarization interferometry [35]. However, this is to our knowledge the first report where the potential use of MB conformational changes upon hybridization are observed and exploited using an evanescent-wave photonic sensor, which will be of great interest for the future development of novel label-free biosensors.

3. Materials and methods

3.1 Photonic sensing structures

For the demonstration of the MB conformational change effects on evanescent wave photonic sensor, we made use of planar integrated nanophotonic technology, due to their multiple advantages: high sensitivity, compactness and high integration level, short time to result, label-free detection, use of very low sample volumes, compatibility with CMOS (Complementary Metal-Oxide-Semiconductor) technology fabrication, etc. [36-38]. Particularly, we developed PBG sensing structures created by periodically introducing a modulation in the refractive index of the photonic structure. Their transduction principle is based on the dependence of their response to changes in the refractive index (RI) of the surrounding medium [39-41]. So, the biorecognition of the target oligonucleotide by the MB occurring on the surface will lead to a variation in the RI distribution and in turn to a shift in the position of the PBG, i.e, the spectral range where the propagation of the light is not allowed owing to the periodicity of the structure, as shown in Figure 3. The enhanced interaction of the optical field with the target analytes, due to the slow-wave effect [42, 43], and their extremely small size, make PBG sensing structures an emerging class of refractive-index-sensitive structures for label-free multiplexed biomolecular sensing applications.
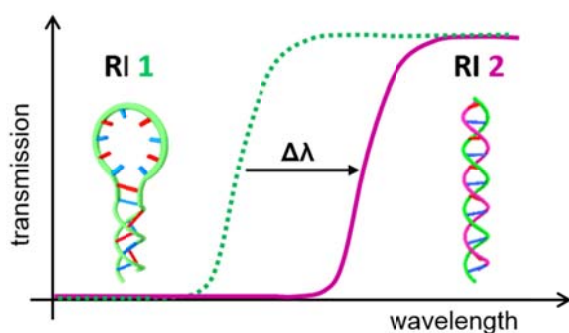

Figure 3 Schematic explanation of the spectral shift of the PBG edge when a biorecognition of the target oligonucleotide by the MB takes place.

Figure 4 schematically depicts the PBG sensing structure used in this work. It consists on a silicon single mode waveguide of height h=220 nm and width w=460 nm, where 50 silicon transversal elements of width w_i=140 nm and length w_e=1500 nm are introduced with a periodicity a=380 nm; the silicon structure is placed on top of a silicon oxide lower cladding. The dimensions of the PBG sensing structure were selected in order to obtain a PBG edge located at a wavelength around 1550 nm when a water upper cladding surrounds the structure, as this is the wavelength range where the interrogation equipment available at our laboratory operates. A 5-elements taper, where the length of the transversal

elements is linearly varied, is also included at the input and the output of the PBG sensing structure in order to improve the light coupling from/to the single mode waveguide.
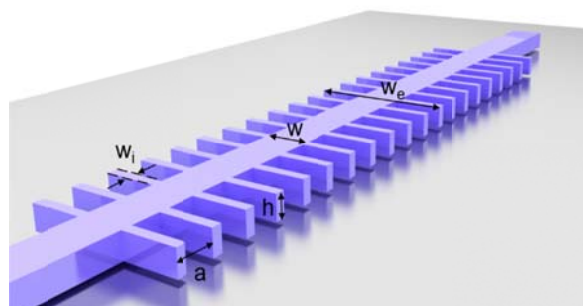

Figure 4 Schematic representation of the selected PBG sensing structure. The periodic silicon photonic structure is placed on top of a silicon oxide lower cladding. Note that the linear access taper is not included in the scheme.

The fabrication of the PBG sensing structures was performed in a standard silicon-on-insulator (SOI) wafer by means of e-beam lithography with an acceleration voltage of 100 keV and inductively coupled plasma etching of the top silicon layer. A scanning electron microscope (SEM) image of a fabricated PBG sensing structure is shown in Figure 5. Four PBG sensing structures were included in a single photonic chip to perform multiplexed detection in order to compare the sensing response for the streptavidin-labeled and the streptavidin-free MB probes at the same time. The chip was accessed at the input and the output via 70 nm-deep shallow etch 1D grating couplers.
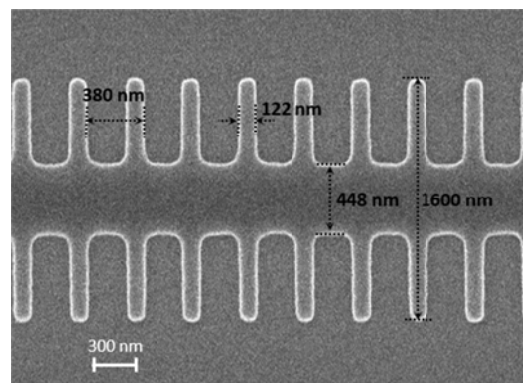

Figure 5 SEM image of a fabricated PBG sensing structure.

3.2 Functionalization

The immobilization of MBs on the photonic structures has to be robust and biocompatible. In this regard, thiol-

ene coupling (TEC) chemistry provides a fast, homogeneous biofunctionalization of the surface under mild conditions [35, 44, 45]. To achieve immobilization, thiolated MBs (5'-3' sequence: SH-ATC GAC ACC CCT ATC ACG ATT AGC ATT AAG *TCG AT; * denotes a modified T to incorporate a biotin moiety, Eurofins Scientific, Luxembourg) were coupled to the previously vinyl-derivatized surface of the PBG structures following a previously optimized protocol [35]. To introduce alkene groups on the photonic structures, the photonic chip was rinsed with ethanol and water and immediately activated with UV-vis irradiation at 254 nm (50 mW·cm^{-2}) for 10 minutes. The chip was then immersed in a 2% solution of vinyltriethoxysilane (Sigma-Aldrich, Germany) in toluene for 2 hours. Then the photonic chip was washed with acetone and air dried. Finally, a water contact angle (WCA) of 76.7±0.1° was measured after curing the chip for 30 minutes at 90 °C, demonstrating functionalization.

Then, the MB probes were immobilized onto the vinyl-functionalized PBG sensing structures by TEC chemistry. Thiolated MB probe solutions (30 nL, 10 µM in ultrapure water) were drop casted on them and left to dry at room temperature. The chip was then irradiated at 254 nm (50 mW·cm^{-2}) for 30 seconds to achieve photoimmobilization. Once the MBs were immobilized, the photonic chip was thoroughly washed with PBS-T (phosphate buffer saline with a 0.5 % tween 20), distilled water and air dried.

Streptavidin was attached to the MBs of two of the PBG structures by depositing a solution of streptavidin (5 µL, 20 ppm in PBS-T) over the desired PBG structures and incubated in a humid chamber to promote the streptavidin-biotin link at room temperature. After, the chip was intensively washed with PBS-T and water to remove any streptavidin unspecifically attached to the MBs.

The target oligonucleotide used for the sensing experiments had the sequence fully complementary to the MB sequence (AUC GAC UUA AUG CUA AUC GUG AUA GGG GUG UCG AU 5' to 3') and was diluted in saline-sodium citrate (SSC) 5× at 0.5 µM concentration.

3.3 Experimental setup

The biofunctionalized photonic sensing chip was assembled with a microfluidic flow cell comprising a bottom holder, where the photonic chip was placed, and a top fluidic lid having a 500 µm-wide, 500 µm-high and 7.5 mm-long rubber channel. The assembled chip was placed on an automated optical readout setup, as shown in Figure 6, able to continuously acquire the transmission spectrum of the PBG sensing structures to monitor their spectral shifting. A wavelength-tunable laser (Keysight 81980A), centered at 1550 nm, was coupled to the access

grating couplers using a fiber aspheric collimator (Thorlabs CFS2-1550-APC) and the light from the output grating couplers was collected with an objective (20X Olympus Plan Achromat, 0.4 NA) and measured using an infrared (IR) camera (Xenics Xeva-1.7-320). The interrogation platform was controlled by a software implemented in LabVIEW able to synchronize the continuous sweep of the laser with the image acquisition of the IR camera via a trigger signal. The target solutions were flown using a syringe pump working in withdraw mode and set to a constant flow rate of 20 µl/min.
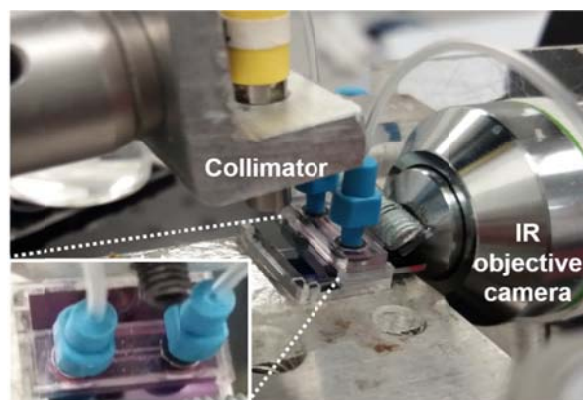

Figure 6 Picture of the assembled photonic sensing chip placed on the interrogation platform and detailed image of the flow cell having the microfluidic channel on its bottom side.

4. Experimental results

An example of transmission spectrum is shown in Figure 7 for one of the biofunctionalized PBG sensing structures on the photonic chip, whose PBG edge is located around 1560 nm.
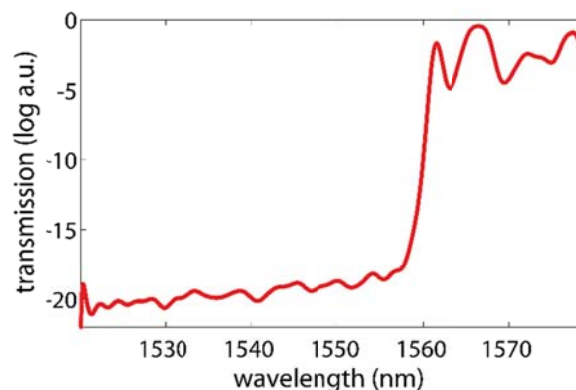

Figure 7 Example of transmission spectrum for one of the biofunctionalized PBG sensing structures.

Figure 8 shows the sensing response, i.e., the spectral evolution of the PBG edge, towards the target oligonucleotide hybridization for the biofunctionalized PBG sensing structures on the chip. The initial baseline was obtained flowing SSC 5× buffer, which was employed as carrier buffer for the target oligonucleotide in the experiments. At t=14 min, a solution of the target oligonucleotide was flown over the sensors, whose recognition by the MB probes produced the shift of the PBG edges of the sensing structures. Finally, an additional cycle of SSC 5× buffer was flown at t=24 min in order to remove any non-hybridized oligonucleotide present in the medium; the PBG edge positions remained unchanged, indicating that hybridization of the target oligonucleotide strand was successful. Note that the experiment was carried out at room temperature and it was stable and constant during the whole process. Unfortunately, one PBG sensing structure biofunctionalized with streptavidin-free MBs was damaged and no output signal was measured.
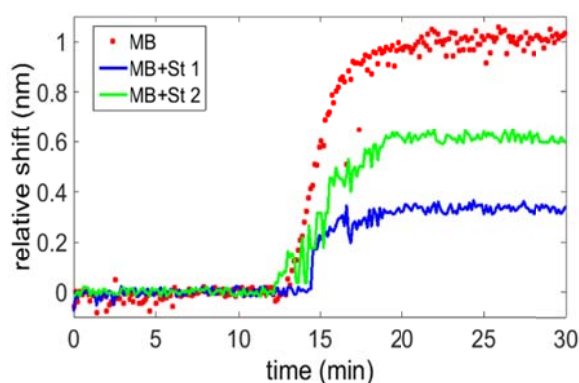

Figure 8 Temporal evolution of the PBG edge position of the sensing structures when the target oligonucleotide strand is flown over the sensors. The sensing response for the PBG structure being biofunctionalized with the streptavidin-free MB probes is depicted with red dots, while the sensing response of the PBG sensing structures being identically biofunctionalized with the streptavidin-labeled MB probes (MB+St 1 and MB+St 2) are depicted with green and blue solid lines.

From Figure 8, it can be observed that very remarkable PBG edge shifts were obtained in all cases for target oligonucleotide detection (from ~350 pm to even ~1000 pm). However, a significantly different sensing response was obtained for the three biofunctionalized PBG sensing structures considered in the experiments, even between those having streptavidin-labeled MB probes. So, in order to determine whether these different responses were due to differences in the biorecognition process by the MB probes or to sensitivity differences of the PBG sensing structures themselves, an additional RI calibration cycle was carried out in order to normalize the sensing responses. In this calibration cycle, the PBG edge shift produced by the change from SSC 5×

buffer to ultrapure water was measured. Table 1 shows the spectral shifts measured for both the target oligonucleotide detection experiment and the RI calibration cycle, while Figure 9 shows the normalized oligonucleotide detection response of the PBG sensing structures when that absolute value of the shift in the calibration cycle was considered (normalized final PBG edge shifts are also indicated in Table 1). Table 1 also includes additional oligonucleotide detection results for other two identical PBG sensing structures biofunctionalized with streptavidin-free MBs (MB 1* and MB 2*) obtained using a different chip in a different experiment [46]. These results are included in order to overcome the problem of having only a single working PBG sensing structure biofunctionalized with the streptavidin-free MB in the original experiment.

Table 1 Measured spectral shifts for the detection of the target oligonucleotide strand and for the RI calibration cycle. The last column indicates the normalized PBG edge shifts for the target oligonucleotide detection experiment. The * mark denotes the

	Oligonucleotide detection (pm)	RI calibration (pm)	Normalized oligonucleotide detection
MB+St 1	345	-1890	0.183
MB+St 2	620	-3230	0.192
MB	1020	-1560	0.654
MB 1*	920	-1390	0.662
MB 2*	1120	-1804	0.621

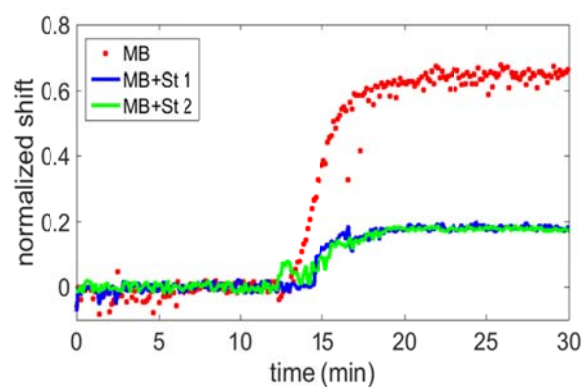results obtained in another experiment using another chip.

Figure 9 Normalized temporal evolution of the PBG edge position of the sensing structures. The normalized sensing response for the PBG structure being biofunctionalized with the streptavidin-free MB probes is depicted with red dots, while the sensing response of the PBG sensing structures being biofunctionalized with the streptavidin-labeled MB probes are depicted with green and blue solid lines.

On one hand, the normalized shifts were identical for the two PBG sensing structures being biofunctionalized with streptavidin-labeled MB probes (~0.19). Therefore, the different shifts previously observed in Figure 8 were attributed to the differences in sensitivity of the PBG sensing structures, probably because of deviations on the fabrication process. On the other hand, significantly different shifts were obtained for the PBG sensing structures being biofunctionalized with the streptavidin-free MB probes (~0.65), thus indicating a different interaction of the MB probe with the evanescent field of the photonic sensing structure when incorporating streptavidin.

In the light of the results obtained from the experiments, it can be observed that the presence of the streptavidin molecule attached to the MB probe produces a significant decrease of the normalized sensing response of the PBG sensing structures, compared with the case of using streptavidin-free MB probes (by a ~3.6× factor). In order to discard that the streptavidin may hamper the recognition of the target oligonucleotide by the MB probe and lead to a lower hybridization yield, fluorophore-labeled oligonucleotide targets were used in the experiments; the fluorescence after hybridization was compared for both MB probes configurations, providing similar results. Thus, we concluded that the difference observed in the photonic measurements was determined by the additional displacement effect produced for the streptavidin-labeled MB probes, as schematically explained in Figure 10. When the streptavidin molecule was displaced, due to the conformational change of the MB, matter was removed from the surface of the photonic sensing structure, what was translated into a backshift of the PBG edge. However, in this case the magnitude of that backshift was smaller than the significantly large positive shift measured for the direct detection of the target oligonucleotide by the streptavidin-free MB probes. So, a smaller positive net shift was obtained when using the streptavidin-labeled MB probes due to the combination of both effects.
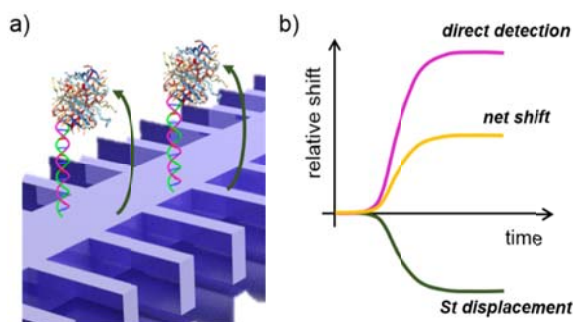

Figure 10 a) Schematic representation of the displacement of the streptavidin from the surface of the PBG sensing structure when the MB changes its conformation due to the hybridization with the target oligonucleotide. b) Schematic representation of the photonic sensor response when streptavidin-labeled MB

probes are used. The final net response is a result of the combination of the positive shift given by the direct recognition of the target oligonucleotide and of the negative shift given by the streptavidin displacement.

5. Conclusion

In this work, we have experimentally observed the influence of the conformational changes of MB probes over evanescent wave photonic sensing structures. This is, to our knowledge, the first time that this effect is reported for this type of optical sensors.

By labeling MB probes with a molecule, it is possible to obtain a sensing response being the combination of both the direct oligonucleotide detection event and the displacement of that molecule produced by the conformational change of the MB. Despite, in this experimental study, the net shift obtained by the combination of these two effects means a reduction of the sensing response compared to the direct detection of the target oligonucleotide (i.e., when no molecule is used), a proper selection of the matter being attached to the MB (e.g., a high refractive index nanoparticle or a bigger size molecule) might induce a higher backshift that significantly dominates the detection process, what might lead to an amplification of the response of the photonic sensing structure.

Another potential application of this effect is to improve the sensitivity towards the detection of very low molecular weight targets, as for example pesticides or antibiotics, whose direct detection provides an extremely low spectral shift. In that case, the negative shift produced by the displacement of the attached molecule/particle will dominate, thus providing a net negative shift significantly higher to that of the direct target detection. Note that for the case of non-oligonucleotide-based targets, the MB probe should be replaced by an aptamer, which also suffers a conformational change upon the recognition of its specific target.

Finally, this effect might be further exploited by a proper design of the photonic sensing structure in order to have several optical modes with different evanescent field profiles, which can interact in a different way with the hybridized target oligonucleotide and with the displaced molecule/nanoparticle [47].

References

[1] P. D. Patel, Trends in Anal Chem **21**(2), 96-115 (2002).

[2] B. Pérez-López, and A. Merkoçci, Trends Food Sci Technol **22**, 625-639 (2011).

[3] G. Zanchetta, R. Lanfranco, F. Giavazzi, T. Bellini, and M. Buscaglia, Nanophotonics **6**(4), 627-645 (2017).

[4] P. Yáñez-Sedeño, L. Agüí, R. Villalonga, and J. M. Pingarrón, Anal Chim Acta **823**, 1-19, (2014).

[5] A. Ricciardi, A. Crescitelli, P. Vaiano, G. Quero, M. Consales, M. Pisco, E. Esposito, and A. Cusano, Analyst **140**, 8068-8079, (2015).

[6] C. S. Huertas, S. Domínguez-Zotes, and L. M. Lechuga, Scientific Reports **7**, 4136 (2017).

[7] P. Muhonen and H. Holthofer, Nephrol Dial Transplant **24**, 1088-1096 (2009).

[8] E. Y. Liu, C. P. Cali, and E. B. Lee, Dis Model Mech **10**, 509-518 (2017).

[9] I. Casanova-Salas, J. Rubio-Briones, A. Fernández-Serra, and J. A. López-Guerrero, Clin Transl Oncol **14**, 803-811 (2012).

[10] A. J. Hopwood, C. Hurth, J. Yang, Z. Cai, N. Moran, J. G. Lee-Edghill, A. Nordquist, R. Lenigk, M. D. Estes, J. P. Haley, C. R. McAlister, X. Chen, C. Brooks, S. Smith, K. Elliott, P. Koumi, F. Zenhausern, and G. Tully, Anal Chem **82**, 6991−6999 (2010).

[11] M. J. Bañuls, V. González-Pedro, C. A. Barrios, R. Puchades, and Á. Maquieira, Bionsens Biolectron **25**(6), 1460-1466 (2010).

[12] A. Sassolas, B. D. Leca-Bouvier, and L. J. Blum, Chem Rev **108**(1), 109-139 (2008).

[13] L. A. Tortajada-Genaro, R. Puchades, and Á. Maquieira, J Pharm Biomed Anal **13**, 614-621 (2017).

[14] J. Escorihuela, M. J. Bañuls, R. Puchades, and Á. Maquieira, Bioconjugate Chem **23**, 2121-2128 (2012).

[15] A. Vainrub, and B. M. Petitt, J Am Chem Soc **125**, 7798-7799 (2003).

[16] S. Tyagi, and F. R. Kramer, Nat Biotechnol **14**, 303-308 (1996).

[17] B. Dubertret, M. Calame, and A. Libchaber, J Nat Biotech **19**, 365-370 (2001).

[18] H. S. Joshi, and Y. Tor, Chem Commun **0**, 549-550 (2001).

[19] T. Heinlein, J. P. Knemeyer, O. Piestert, and M. J. Sauer, Phys Chem B **107**, 7957-7964 (2003).

[20] D. J. Williams and K. B. Hall, Biochemistry **35**, 14665-14670 (1996).

[21] P. V. Riccelli, F. Merante, K. T. Leung, S. Bortolin,R. L. Zastawny, R. Janeczko, and A. S. Benight, Nucleic Acid Res **29**, 996-1004 (2001).

[22] Z. Mei, and L. Tang, Anal Chem **89**, 633-639 (2017).

[23] Q. Guo, Z. Bai, Y. Liu, and Q. Sun, Biosens Bioelectron 77, 107-110 (2016).

[24] A. Dodge, G. Turcatti, I. Lawrence, N. F. de Rooij, and E. Verpoorte, Anal Chem **76**, 1778-1787 (2004).

[25] D. Van Lierop, K. Faulds, and D. Graham, Anal Chem **83**(15), 5817-5821 (2011).

[26] A. Kotnala and R. Gordon, Biomed Opt Express **5**(6), 1886-1894 (2014).

[27] F. Wei, B. Sun, W. Liao, J. Ouyang, and X. Sheng Zhao, Biosens Bioelectron **18**(9), 1149-1155 (2003).

[28] S. Li, Y. Wang, C. Gao, S. Ge, J. Yu, and M. Yan, Electroanal Chem **759**, 38-45 (2015).

[29] X. Miao, X. Guo, Z. Xiao, and L. Ling, Biosens Bioelectron 59, 54-57 (2014).

[30] V. Rai, Y. T. Nyine, H. C. Hapuarachchi. H. M. Yap, L. C. Ng, and C-S. Toh, Biosens Bioelectron **32**, 133-140 (2012).

[31] J. Li, Y. Liu, X. Zhu, G. Chang, H. He, X. Zhang, and S. Wang, ACS Appl Mater Interfaces **9**, 44231-44240 (2017).

[32] K. Wang, Z. Tang, C. J. Yang, Y. Kim, X. Fang, W. Li, Y. Wu, C. D. Medley, Z. Cao, J. Li, P. Colon, H. Lin, and W. Tan, Angew Chem Int Ed **48**(5), 856-870 (2009).

[33] J. Zheng, R. Yang, M. Shi, C. Wu, X. Fang, Y. Li, J. Li, and W. Tan, Chem Soc Rev **44**(10), 3036-3055 (2015).

[34] E. A. Bayer, and M. Wilchek, Methods in enzymology 184, 49-51 (1990).

[35] D. Gónzalez-Lucas, M. J. Bañuls, J. García-Rupérez, and Á. Maquieira, Microchim Acta **184**, 3231-3238 (2017).

[36] X. Fan, I. M. White, S. I. Shopova, H. Zhu, J. D. Suter, and Y. Sun, Anal Chim Acta **620**, 8-26 (2012).

[37] M. S. Luchansky, and R. C. Bailey, Anal Chem **84**, 793-821 (2012).

[38] M. C. Estevez, M. Alvarez, and L. M. Lechuga, Laser Photonics Rev **6**, 463-487 (2012).

[39] D. Conteduca, F. Dell'Olio, C. Ciminelli, and M. N. Armenise, Appl Opt 54(9), 2208-2217 (2015).

[40] A. K. Goyal, and S. Pal, Optik 126 (2), 240-243 (2015).

[41] P. Prabhathan, and V. M. Murukeshan, Journal of the Indian Institute of Science 94 (3), 273-282 (2014).

[42] M. L. Povinelli, S. G. Johnson, and J. D. Joannopoulos, Opt Express **13**, 7145-7159 (2005).

[43] J. García, P. Sanchis, A. Martínez, and J. Martí, Opt. Express **16**, 3146-3160 (2008).

[44] J. Escorihuela, M-J. Bañuls, S. Grijalvo, R. Eritja, R. Puchades, and Á. Maquieira, Bioconjugate Chem **25**(3), 618-627 (2014).

[45] D. Winrich, M. Köhn, P. Jonkheijm, U. Westerlind, L. Dehmelt, H. Engelkamp, P. C. M. Christianen, J. Kuhlmann, J. D. Maan, D. Nüsse, H. Schröder, R. Wacker, E. Voges, R. Breinbauer, H. Kunz, C. M. Niemeyer, and H. Waldmann, ChemBioChem **11**, 235-247 (2010).

[46] Á. Ruiz-Tórtola, F. Prats-Quílez, D. González-Lucas, M-J. Bañuls, Á. Maquieira, G. Wheeler, T. Dalmay, A. Griol, J. Hurtado, and J. García-Rupérez, Biomed Opt Express **9**(4), 1717-1727 (2018).

[47] C. S. Huertas, D. Fariña, and L. M. Lechuga, ACS Sens **1**(6), 748-756 (2016).